PFG 2016 / 2, 0057 – 0073
Stuttgart, April 2016

Article

Dense Image Matching vs. Airborne Laser Scanning – Comparison of two methods for deriving terrain models

CAMILLO RESSL, Vienna, Austria, HERBERT BROCKMANN, Koblenz, GOTTFRIED MANDLBURGER & NORBERT PFEIFER, Vienna, Austria

Keywords: laser scanning, image matching, terrain, accuracy

Summary: In this article the performance of dense image matching (DIM) is investigated regarding its capability to yield terrain data, especially close to free-flowing water ways. Therefore, over two study areas aerial images with ground sampling distances 10 cm and 6 cm, respectively, are used for matching with the software packages Match-T (Trimble) and SURE (nframes). The matching results over areas with varying vegetation density (open grassland, loose and dense vegetation) are then compared with ALS reference data. Two parameters are investigated: (a) the terrain coverage; i.e. the percentage of the terrain covered by the matching results; and (b) the height accuracy of the matching results in the terrain class. The results show that DIM can only deliver terrain data in areas with no or very loose vegetation. Additionally, it was found that in the case of open grassland the DIM terrain heights were systematically higher by 10 cm compared with the ALS terrain heights. This is caused by the fact that ALS can penetrate the vegetation to some extent whereas matching occurs on top of the grass. The very good height accuracy (as standard deviation) obtainable by DIM, which is only slightly worse than the ALS accuracy (6.5 cm vs. 4.5 cm), is encouraging. Motivated by these results new possible applications arise for the respective authorities (the German Federal Institute of Hydrology and the German Federal Water and Shipping Administration), e.g. capturing dry fallen areas of free flowing rivers during documentation at low water levels.

Zusammenfassung: *Vergleich von Bild-Matching und Laserscanning zur Ableitung von Geländemodellen.* In diesem Aufsatz wird untersucht, in wie weit das Matching von digitalen Bildern für die Ableitung von digitalen Geländemodellen speziell im Bereich von freifließenden Bundeswasserstraßen verwendet werden kann. Dafür wird für Luftbilder über zwei Untersuchungsgebieten (Bodenpixelgröße 10 cm bzw. 6 cm) ein Matching mit zwei kommerziellen Programmen (Match-T (Trimble) und SURE (nframes)) durchgeführt. Die sich ergebenden Matching-Ergebnisse werden in Bereichen mit unterschiedlicher Vegetationsdichte (offene Wiese, lockere und dichte Vegetation) mit Laserscanning-Referenzdaten verglichen. Zwei Parameter werden dabei untersucht: (a) die Geländeabdeckung, d. h. der Prozentsatz der Geländefläche, der durch die Matching-Ergebnisse abgedeckt wird; und (b) die Höhengenauigkeit der Matching-Ergebnisse in der Gelände-Klasse. Die Ergebnisse zeigen, dass per Bild-Matching Geländehöhen nur in Bereichen mit keiner oder nur lockerer Vegetation bestimmt werden können. Zusätzlich hat sich gezeigt, dass auf offenen Wiesen die Matching-Höhen systematisch um 10 cm höher als die ALS-Höhen liegen. Das ist eine Folge davon, dass das Lasersignal die Vegetation durch Lücken im Blattwerk zu einem gewissen Teil durchdringen während das Matching nur an den Grasspitzen erfolgen kann. Bemerkenswert ist die sehr gute Höhengenauigkeit (gemessen als Standardabweichung), die mithilfe von Bild-Matching erreicht werden kann. Sie ist mit 6.5 cm nur geringfügig schlechter als die ALS-Genauigkeit von 4.5 cm. Für die verantwortlichen Behörden (Bundesanstalt für Gewässerkunde, sowie Wasser- und Schifffahrtsverwaltung des Bundes) zeigen diese Ergebnisse neue mögliche Anwendungen auf, z.B. die Erfassung von trocken gefallenen Bereichen an Fließgewässern im Rahmen von Niedrigwasserdokumentationen.

www.schweizerbart.de
DOI: 10.1127/pfg/2016/0288
1432-8364/16/0288 $ 4.25

1 Introduction

Over the past 15 years airborne laser scanning (ALS) was generally preferred over stereo photogrammetry for acquiring data for digital terrain models. This is primarily caused by the ability of ALS to penetrate vegetation and yield measurements on the ground (Baltsavias 1999, Petzold et al. 1999).

The same time span, however, showed also two major advancements in photogrammetry: a) the development of digital aerial cameras (Leberl et al. 2012), which allow a complete digital workflow, very high image forward overlaps and small ground sampling distances (GSD), and b) the development of dense image matching techniques (DIM), which enable the automatic generation of dense 3D point clouds from overlapping images with a resolution close to the GSD (Hirschmüller 2008).

Many articles have been published on the DIM-based derivation of digital surface models (DSMs) and their quality evaluation using ALS reference data, e.g. Vastaranta et al. (2013), Haala & Rothermel (2012), Xiao et al. (2012), Haala et al. (2010). However, the usage of DIM for digital terrain models (DTM) has not been investigated much - especially not in vegetated areas. In Bauerhansl et al. (2004) vegetation was considered but only sparse matching was applied to scanned analogue images, leading to unsatisfying results in wooded areas.

Motivated by the mentioned advancements in photogrammetry the German Federal Institute of Hydrology (Bundesanstalt für Gewässerkunde, BfG) in cooperation with the German Federal Water and Shipping Administration (Wasser- und Schifffahrtsverwaltung des Bundes, WSV) and the Department of Geodesy and Geoinformation, TU Wien, initiated a pilot project to investigate the practical performance of DIM for the derivation of a DTM-W (digital terrain model of watercourses). The DTM-W is an important dataset in particular for addressing hydraulic and hydrological issues. It represents the ground of the flow-effective riparian area of a waterway as well as the riverbed with a typical resolution of 1 m × 1 m. The main objective of this project was to clarify whether DIM can be used as a cost-effective alternative to ALS for data collection with at least 4 points per m^2 for processing and updating the DTM-W of the forelands and the dry fallen parts of the littoral zone (during low water situations).

This article presents the main technical outcomes of these investigations. First a brief description of ALS and DIM is given in section 2. The results obtained at two representative study areas (Weser/Bad Karlshafen and Elbe/Klöden) are presented in sections 3 and 4 using profiles, ground coverage and height accuracy. Finally, section 5 draws the main conclusions.

2 Methods of Data Acquisition

2.1 *Airborne Laserscanning (ALS)*

ALS applies an active polar multi-sensor system (Wehr & Lohr 1999, Shan & Toth 2008). A scanner is mounted on a flying platform and emits usually infrared laser pulses. Each pulse interacts with various objects along its path, e.g. leafs, twigs, bushes and ground. Each of these illuminated objects scatters the emitted pulse to some extent, causing a part of it to return as echo to the detector of the scanner. The respective time of flight allows to determine the distance between the scanner and each object. The 3D coordinates of these objects result from the polar scanner measurements (deflection angle and range) and the position and rotation of the sensors (measured using a global navigation satellite system (GNSS) and an inertial navigation system). Consequently, a single sight to an object point is sufficient to determine that point's 3D coordinates. Therefore, the gaps in the canopy, through which points on the ground are measured, can be quite small.

2.2 *Dense Image Matching (DIM)*

Image matching is based on the photogrammetric reconstruction principle. In this case, each object point must be visible in at least two images. Each image point and the respective projection centre define a viewing ray. Provided the interior orientation (principal distance, principal point, lens distortion) and the exterior orientation (spatial location and rotation of the image) are known, the coordinates of the object point can be reconstructed using the spatial intersection of the viewing rays.

Nowadays the term *matching* is often used for the whole process of image point extraction, searching for corresponding points in overlapping images and spatial intersection. Matching, originally, just referred to the 2nd step (Vosselman et al. 2004): the automatic search for correspondences (in two images). The classical approaches were feature based matching (FBM) and area based matching (ABM). Both approaches are *local* in the sense that each correspondence is found independently of already established correspondences in the neighbourhood. In the case of ABM an additional locality is introduced because a small correlation window is used, which inherently assumes that all pixels in that window stem from object points at the same depth. This assumption is clearly not valid e.g. in the case of depth discontinuities and occlusions. These classical approaches are *sparse* in the sense that only a small fraction of the pixels in each image generates 3D points.

In contrast to this, *dense image matching* (DIM) tries to find correspondences for every n-th pixel. For n=1 the resulting 3D point cloud will have a point distance identical to the GSD of the images. Nowadays the GSD of aerial images is typically in the range of 5 cm–20 cm.

In recent years semi-global matching (SGM) was introduced (Hirschmüller 2008) and disseminated (Rothermel et al. 2012). For SGM, first, the colour values of the pixels are transformed into a more robust domain, e.g. using census transformation (Zabih & Woodfill 1994). Afterwards SGM performs dense image matching for every pixel by minimising the difference of the transformed values of the pixel in the left and the corresponding pixel in the right image. In order to improve the robustness of this approach and to bridge areas of poor texture SGM applies a smoothness constraint, which favours correspondences that produce neighbouring points having the same depth. Both, the difference of the transformed pixel values and the smoothness constraint, are combined in a weighted sum. This sum is then minimised as an energy function. Depending on these weights the smoothness constraint may be violated in case of depth changes, e.g. at roofs or tilted planes, because there, the pixel value difference can be dramatically reduced for non-neighbouring pixels.

Because two image rays to an object point are required to determine that point's 3D coordinates, matching images of vegetated areas will primarily deliver points on the visible top of the canopy. Matching points on the ground through gaps in the canopy is difficult for two reasons: (i) generally, it is not very likely that the same point on the ground will be visible through the canopy in images made from two different projection centres, (ii) even if this happened, dark shadows on the forest floor might cause bad image texture. Consequently, at such locations matching is prevented at all or the smoothness constraint takes over and keeps the heights at the dominant visible object (the canopy). However, with increasing size of the gaps and decreasing density of the vegetation, chances will grow that matching can deliver points on the ground.

2.3 *Used Matching Software*

In this study the following two commercially available software packages were used: nframes SURE (version 20140716_2245) and Trimble Match-T (version 5.5). Both apply an SGM-based approach (Rothermel et al. 2012 and Trimble 2014).

2.3.1 SURE

SURE uses each image as so-called *base image*. The software matches every pixel in this base image with pixels from each directly neighbouring image (of the same strip and the neighbouring strips) and then computes a multi-image-based spatial intersection. At the end the point clouds obtained for each base image are merged by a median-based fusion to form a grid of the entire project area. In this way the high image overlaps are exploited very well. SURE offers a scenario parameter which defines the actual matching parameters, controling e.g. the applied census transformation, the considered disparity ranges, and the selected image pairs based on acceptable viewing angles. The following scenario settings were tested: DEFAULT, AERIAL8080 and OBLIQUE.

2.3.2 Match-T

Match-T uses an SGM implementation which internally is termed *cost based matching* (CBM). The resulting point cloud, however, is not the set of points that were originally computed by spatial intersection but an interpolated grid, with a grid spacing that defaults to three times the GSD. In the version 5.4, calling Match-T with all images of a block worked in the following way: Based on the forward and cross overlaps of the images a certain structure of regions is established. Each region is covered by a single pair of consecutive images, whose matching results are solely responsible for the heights in that particular region. In this way each height in the final model of the entire project area is eventually derived from two images only. The possibly very large image overlaps are not exploited (e.g. at 80 % forward overlap each object point is mapped into five images). Additionally, all matched points have practically the same height accuracy – the one stemming from the image pair with the smallest base.

Therefore, in the version 5.5 a new option called *UAS* was included, which better exploits high image overlaps that typically occur with images from unmanned aerial systems. However, the manual of Match-T does not explain how this UAS method actually works.

Alternatively this limited exploitation of high image overlaps can also be avoided by user interaction. We implemented a workflow by calling Match-T in a batch mode were each matching job consists of only two images and the set of all jobs comprises all possible image pairs (within a selected range of image overlaps). In the end all pair-wise grid results are fused by computing the median of all heights per grid cell. In case of a flight with 80 % forward overlap each object point is mapped into five images and thus is contained in four image pairs with 80 % overlap. If the strips were flown with 50 % cross overlap each point appears in two strips. Then in total each point is contained in eight image pairs and during the fusion the median of eight heights is computed. In sections 3 and 4 the used range of image overlaps for this fusion method will be encoded in the name of the Match-T results; e.g. (85705570 q) means that the result was derived using all image pairs in the same strip with overlaps 85 %, 70 % and 55 %, as well as image pairs covering two strips with overlap 70 %.

2.4 *Study Areas*

ALS and image data were available for two project regions in Germany. In each region a small study area with a varying vegetation density was selected.

Over project region **Weser/Bad Karlshafen** (total area 565 km^2) the images were acquired using a Zeiss DMC-II (GSD: 10 cm, forward overlap: 85 %, cross overlap: 70 %, PAN+RGB, date: April 2013). The laser data were acquired using a Riegl LMS-Q 560 (point density: 6 points/m^2, date: March 2011). Both flights occurred in early spring before foliation. The selected study area, see Fig. 1, has a size of 1500 m × 1500 m and is covered by 91 images. This area is of interest for three reasons: (i) heterogeneous land cover (high, low, dense and loose vegetation, settlement, water), (ii) rough and smooth surface, (iii) flight parameters (very high overlap and medium sized GSD). DIM grids were generated from the PAN images using SURE with a grid width of 10 cm. The Match-T products were generated with a grid width of 25 cm. The SURE grid is visualised in Fig. 3a.

Over project region **Elbe/Klöden** (total area 34 km^2) the images were acquired using a Vexcel UltraCam X (GSD: 6 cm, forward overlap: 80 %, cross overlap: 70 %, PAN+RGB(I), date: April 2013). The laser data were acquired simultaneously using an Optech ALTM Gemini (point density: 4 points/m^2). The flight occurred in early spring before foliation. The selected study area, see Fig. 2, has a size of 1000 m × 1000 m and is covered by 98 images. This area is of interest for three reasons: (i) smooth and homogenous coverage (grassland), (ii) simultaneous image and laser acquisition, (iii) flight parameters (very high overlap and small GSD). Note that the ALS data do not fully cover the study area; this is later considered by a mask. DIM grids generated from the PAN images using SURE have a grid width of 7 cm, the ones using Match-T have a grid width of 15 cm. The SURE grid is visualised in Fig. 3b.

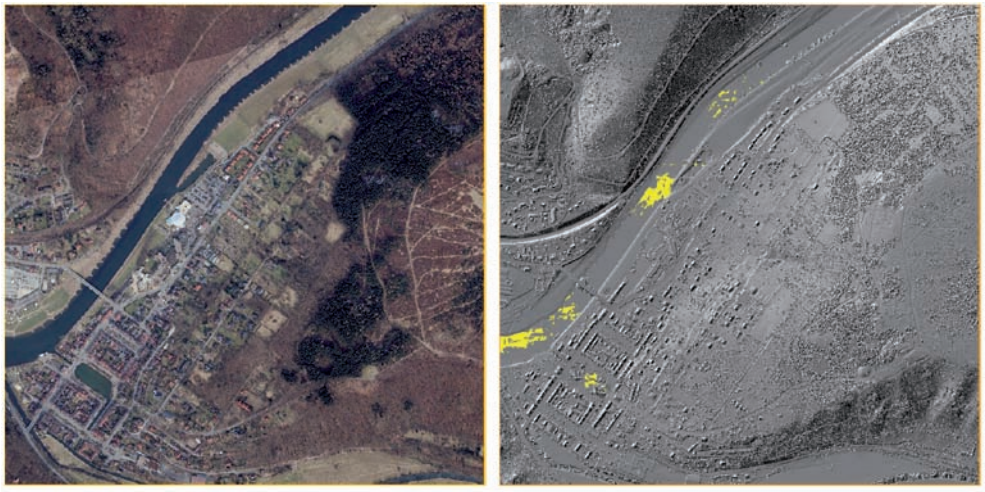

(a) Orthophoto (b) ALS-DSM shading

Fig. 1: The selected study area Weser/Bad Karlshafen. East-west extension 1500 m. Yellow = no data. The ALS-DSM used only the last echoes. For the orthophoto-mosaic no colour correction was applied.

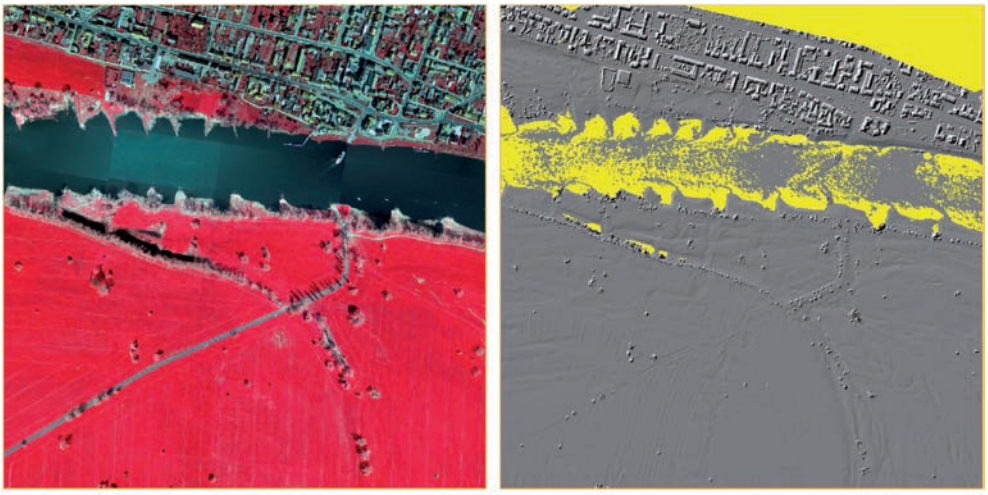

(a) Orthophoto (b) ALS-DSM shading

Fig. 2: The selected study area Elbe/Klöden. East-west extension 1000 m. Yellow = no data. The ALS-DSM used only the last echoes. For the orthophoto-mosaic the false-colour composite images were used and no colour correction was applied.

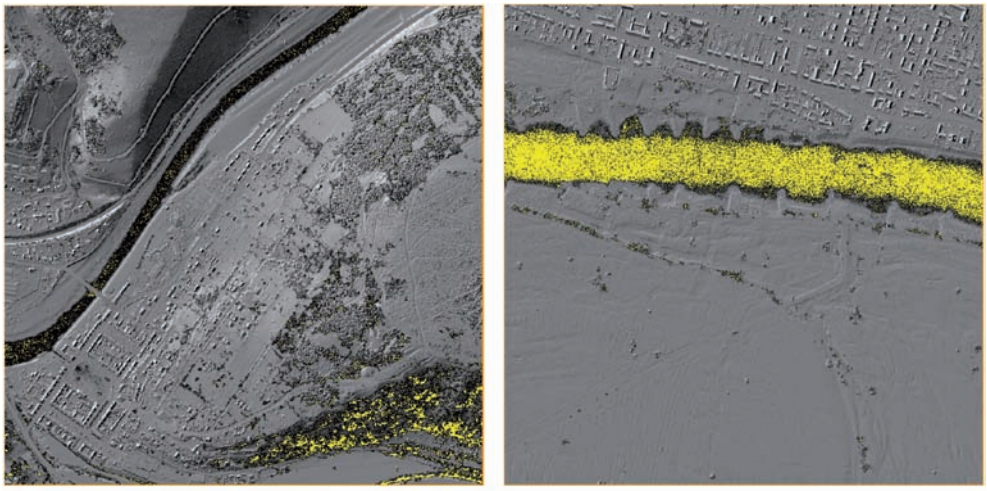

(a) Weser (b) Elbe

Fig. 3: Shadings of the SURE grids in study area Weser (left) and Elbe (right). Yellow = no data. Note that in water areas DIM either delivers wrong heights or no data at all.

For both project regions the ALS data were acquired in accordance with the guideline of the public mapping authorities (AdV 2013). These guidelines prescribe that at least 95 % of the height differences between ALS and check points should be smaller than 15 cm in flat to undulating terrain and smaller than 30 cm in steeper areas distributed over all land cover classes. The accuracy of the ALS-DTMs in the two study areas does not only conform with these specifications, it actually surpasses them – as it is documented using reference data. For the DTM-W over the project region Weser with 565 km^2 5170 check points were measured and 99 % of their differences meet the above mentioned specifications. For the project region of Elbe with 34 km^2 22210 check points were used and 97 % fulfil the requirements mentioned above.

For both project regions the images were oriented using the standard procedure of GNSS assisted aerial triangulation, during which automatic tie points were extracted with an accuracy of 0.1 pixel. Depending on their multiplicity the estimated height accuracy of the tie points ranges from 2 cm to 11 cm (Weser) and 1 cm to 5 cm (Elbe).

In section 3 the applied methods and results are presented for study area Weser. The same methods are applied in study area Elbe in section 4, where only the results are presented.

3 Applied Methods and Results for Study Area Weser

The analysis of the matching results is done qualitatively using profiles and quantitatively by considering two parameters: (a) the **terrain coverage**; i.e. the percentage of the terrain covered by the matching results; and (b) the **height accuracy** of the matching results in the terrain class. The reference for both parameters is the DTM derived from the ALS data.

3.1 *Profiles*

Fig. 4a shows a profile through *dense vegetation*. ALS delivers echoes from the top of the trees, within the vegetation and from the ground. As mentioned at the end of section 2.2, DIM only delivers points at the top of the trees in the vegetated parts. Only in clearings DIM can deliver points on the ground.

Fig. 4b shows a profile through *loose vegetation*. Again ALS delivers echoes from the top of the trees, within the vegetation and from the ground. However, DIM practically only delivers points on the ground. Obviously, the gaps

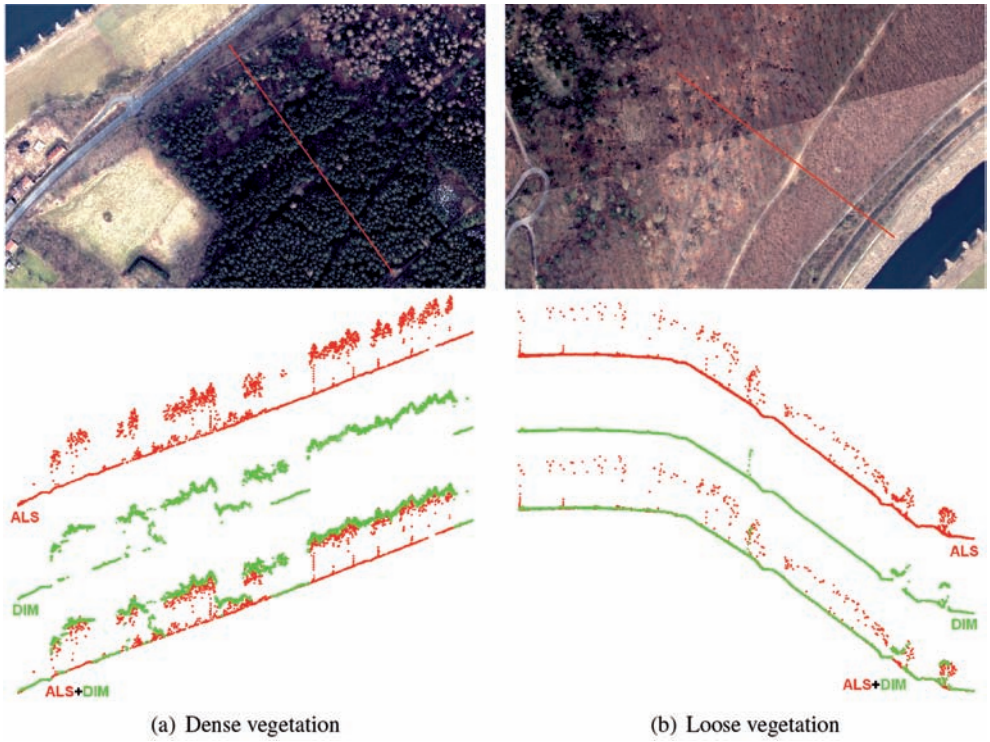

Fig. 4: Two profiles in study area Weser. The ALS points are shown in red, the DIM points (from SURE (OBLIQUE)) in green. In the last row the DIM points are superimposed on the ALS points. The east west extension of both orthophoto sections is about 500 m. The vertical direction of the profiles is magnified by a factor of 1.5.

in the vegetation are wide enough and thanks to the smoothness constraint, DIM is not disturbed by the loosely distributed trees with no or only little foliage.

3.2 *Classification of Terrain Points*

As shown in the previous section, the success rate of DIM for delivering points on the ground is influenced by the density of the vegetation. Therefore, the ALS-DTM is used as the reference for the subsequent classification of individual points into terrain and off-terrain points. This DTM is derived from the given ALS data using all last echoes by means of robust interpolation (KRAUS & PFEIFER 1998) with a grid width of 0.5 m. The DTM was visually analysed using a shaded relief map to ensure that it is free of gross errors.

The classification of ALS and DIM points into terrain points and off-terrain points is performed using their distance ΔZ to the ALS-DTM.

3.2.1 ALS Classification

Fig. 5 shows the histogram of the differences ΔZ of the last echos to their DTM in study area Weser – limited to the interval $\text{abs}(\Delta Z) < 20\,\text{cm}$. The ordinary standard deviation $\sigma_{\Delta Z}$ of these differences is 4.7 cm. The histogram is very similar to a Gaussian distribution with zero mean. Based on that distribution the robust standard deviation σ_{MAD} is 3.0 cm[1]. The difference between these two dispersion values shows that bigger differences occur slightly

[1] σ_{MAD} is a robust estimator for the standard deviation of a Gaussian distribution derived as $\sigma_{MAD} = 1.4826 \cdot MAD$; where MAD is the median of absolute differences (with respect to the median) derived from all values.

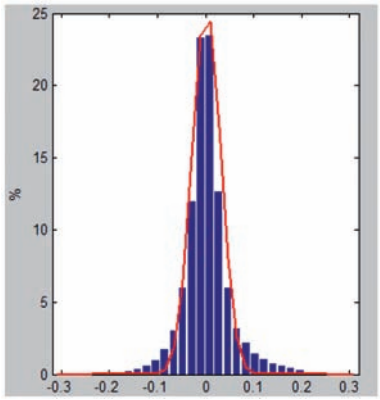

Fig. 5: Histogram of the height differences ΔZ (in m) of the last echos to the ALS-DTM in study area Weser; limited to abs(ΔZ) $<$ 20 cm. A Gaussian distribution with zero expectation and standard deviation 4 cm is drawn in red.

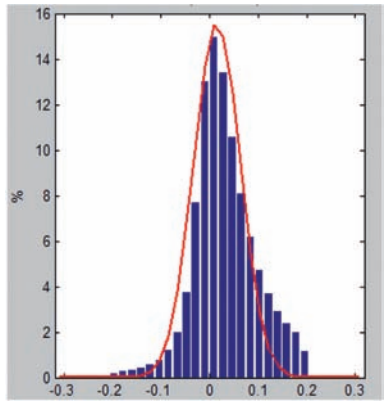

Fig. 6: Histogram of the height differences ΔZ (in m) of the SURE grid (OBLIQUE) to the ALS-DTM in study area Weser; limited to abs(ΔZ) $<$ 20 cm. A Gaussian distribution with expectation 1.5 cm and standard deviation 4.8 cm is drawn in red.

more often than one would expect from a Gaussian distribution. This is a phenomenon that often occurs with real data. It can be explained by the mixture of ΔZ groups with different dispersions. ΔZ values in smooth areas (streets, parking lots) will have very small standard deviations, whereas ΔZ values in rough areas (forest floor) will have bigger standard deviations. The mean is always zero, thus the mixture of these different ΔZ groups will produce a monomodal distribution with a steeper peak.

All last echoes with abs(ΔZ) $<$ $\Delta Z_{\max}$, for a certain threshold $\Delta Z_{\max}$, are classified as terrain. Because the histogram is very similar to a Gaussian distribution we adopt the three-sigma-rule, which is thus fulfilled by $> 99\,\%$ of the terrain points; i.e. it is very unlikely that a terrain point has a ΔZ larger than this threshold. We use the value $\Delta Z_{\max} = 3 \cdot \sigma_{\Delta Z} \approx 15$ cm. In order to evaluate the effect of this choice on the quantitative results, we apply also the $\Delta Z_{\max}$ values 10 cm (based on three times σ_{MAD}) and 20 cm (the whole range considered for the histogram).

3.2.2 DIM Classification

The DIM points are classified also by their height differences ΔZ with respect to the ALS-DTM. Fig. 6 shows the ΔZ histogram for the result of SURE (OBLIQUE) limited to abs(ΔZ) $<$ 20 cm. All DIM variants produce histograms similar to that figure. The negative side of that histogram shows a Gaussian-like shape which therefore justifies cutting off the histogram at 20 cm. As a visual aid the figure also displays a Gaussian distribution with 1.5 cm expectation and a standard deviation of 4.8 cm. It is clearly visible that the histogram is skewed towards the right. This is primarily caused by matching errors that appear as small transitions at height discontinuities (e.g. at cars; see Fig. 7).

In study area Weser the image flight occurred two years later than the ALS flight. In order to compensate for possible terrain changes the following actions were taken. Negative terrain changes like excavations are considered by adapting the classification interval to $[-150, 20]$ cm for the entire area. All DIM points within this interval are classified as terrain. Positive terrain changes, e.g. mounds, can not be considered by enlarging the classification interval to the positive side, because then also many off-terrain points would be classified as terrain. To consider the positive terrain changes, a mask was manually digitized that excludes these parts of the study area from the investigation. Additionally, this mask considers all locations at which DIM can not measure the

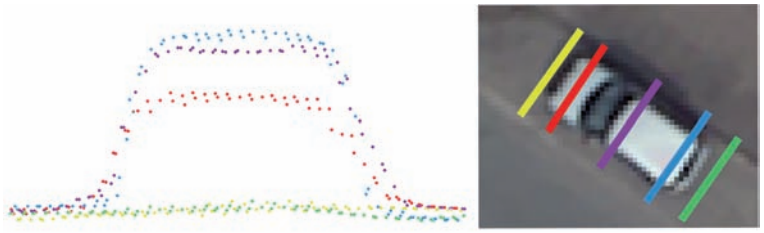

Fig. 7: Five profiles through a car in the SURE grid (OBLIQUE). Small transitions between street and car are clearly visible. The car length is about 3.5 m, its height above the street is about 1.3 m.

Tab. 1: Terrain coverage of the ALS and DIM points in study area Weser. 'abs.' is the absolute count of raster cells classified as terrain. 'rel.' is that count in relation to the count of raster cells ($4 \cdot 10^6$) in the whole study area. The raster width is 75 cm. The ALS points were classified using the interval $[-15, 15]$ cm, the DIM points using $[-150, 20]$ cm.

Method	abs.	rel. [%]
ALS	3283901	82.1
SURE (OBLIQUE)	2583479	64.6
SURE (DEFAULT)	2487792	62.2
SURE (AERIAL8080)	2456907	61.4
Match-T (UAS)	2263574	56.6
Match-T (85705570q)	2276512	56.9

terrain because of e.g. parking cars or because a new house was built after the ALS flight.

Note that because the distribution of the height differences is skewed this classification interval will tend to classify a bit too many DIM points as terrain. However, as we will see later in section 3.3, ALS still has a much larger degree of terrain coverage and therefore the general result is not affected by this tendency.

3.3 *Terrain Coverage*

For determining the degree of terrain coverage a raster with a certain cell size *cs* is defined in the study area. A raster cell is classified as terrain if it contains at least one terrain point. The degree of terrain coverage is then computed (i) absolutely using the number of cells that are classified as terrain and (ii) relatively using the ratio of that absolute number to the area size of the entire study area.

The cell size *cs* was chosen based on the density of the last echo points, which is 6 points/m^2. This corresponds to a point distance of 42 cm and thus would suggest a cell size of 50 cm. Because of the variations in the sampling during laser scanning, some of these cells would not contain a single point and thus the terrain coverage for ALS would be unrepresentatively small. However, within such empty cells the heights could be interpolated easily from the points in the neighbouring cells, indicating that it is not necessary to demand an ALS point every 50 cm. Therefore, the cell size *cs* = 75 cm is chosen.

For this analysis all water areas are masked out. For this mask the union of the areas delineated as water in the ALS data (2011) and in the DIM data (2013) is computed. Thus, any raster cell that is within a water area in any of the delineation sets is excluded from the investigation, even if it was previously classified as terrain. In this way different water levels at both flight dates are compensated. Furthermore, in this mask the terrain changes between both dates mentioned in section 3.2.2 are integrated.

This method for determining the terrain coverage is applied to the previously classified ALS and DIM points. Tab. 1 contains the results. We see that for the whole study area Weser,

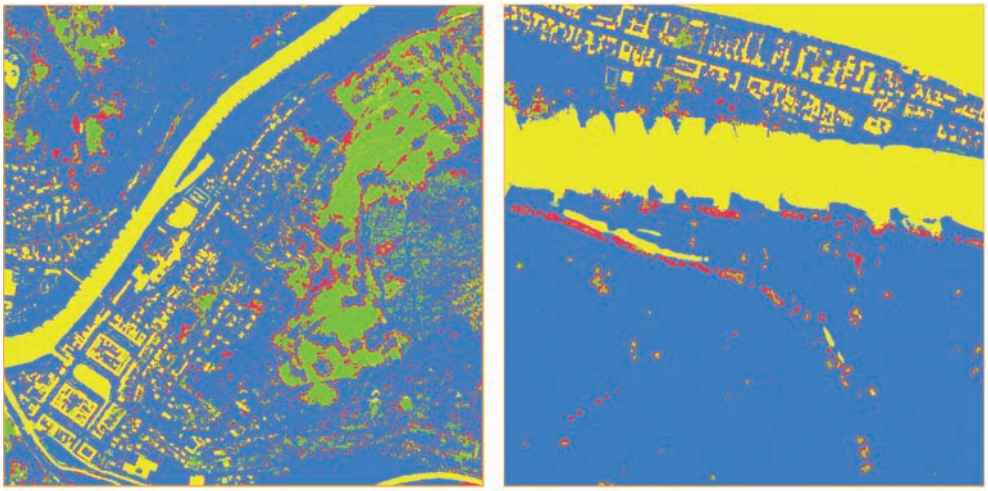

(a) Weser (b) Elbe

Fig. 8: Superimposition of the terrain coverages in study area Weser (left) and Elbe (right). Blue: Match-T + SURE + ALS, red: SURE + ALS, green: ALS. Yellow = Off-terrain or masked.

ALS gives a terrain coverage of 82 %, SURE of 65 % and Match-T of 57 %. ALS has the ability to penetrate vegetation and thus may serve as reference for the terrain coverage that can be achieved. In relation to that SURE delivers a quality of $65/82 = 78\,\%$, and Match-T a quality of $57/82 = 69\,\%$.

As mentioned in section 3.2.1 we also tested the intervals $[-10, 10]$ cm and $[-20, 20]$ cm for the ALS terrain classification. They result in relative terrain coverages of 81 % and 83 %, respectively. This shows that the choice of the classification interval has little influence on the ALS terrain coverage and we thus stick to the result obtained for the interval $[-15, 15]$ cm.

Fig. 8a shows a superimposition of the terrain coverage results for the entire study area Weser and Fig. 9b shows the result for a small section. The terrain coverage of Match-T (85705570 q) is shown in blue, below that is the result of SURE (OBLIQUE) in red and below that is the ALS result in green. Practically at each location where Match-T can deliver terrain heights so does SURE, and at each location where SURE can deliver so does ALS. Summarising, in red areas Match-T fails in comparison with SURE, and in green areas SURE fails in comparison with ALS.

It is clearly visible that in open areas SURE is able to deliver terrain heights closer to nearby off-terrain objects than Match-T – but not as close as ALS. It is also apparent that in dense or high vegetation areas only ALS can deliver terrain heights.

In contrast to SURE, Match-T does not have any no-data areas. The explanation could be that Match-T is less strict in the acceptance of matched or interpolated heights than SURE.

3.4 *Height Accuracy*

The following two statistical values are computed for the height differences ΔZ: a location parameter, which measures a constant shift (e.g. caused by differences in the geodetic datum or by penetration depth) and a dispersion value, which measures the random deviations with respect to that location parameter. Both values are determined using the mentioned ΔZ histograms; see Figs. 5 and 6. Tab. 2 contains the following values for ALS and all DIM variants:

- The usual choices for the location parameter are mean or median. For real data generally the median is preferred, because it is more robust against blunders. In the present case the skewness in the histogram of ΔZ for DIM causes a slight displacement of the median. Therefore, also the mode is reported. The mode denotes the difference value ΔZ with the largest frequency, which, however,

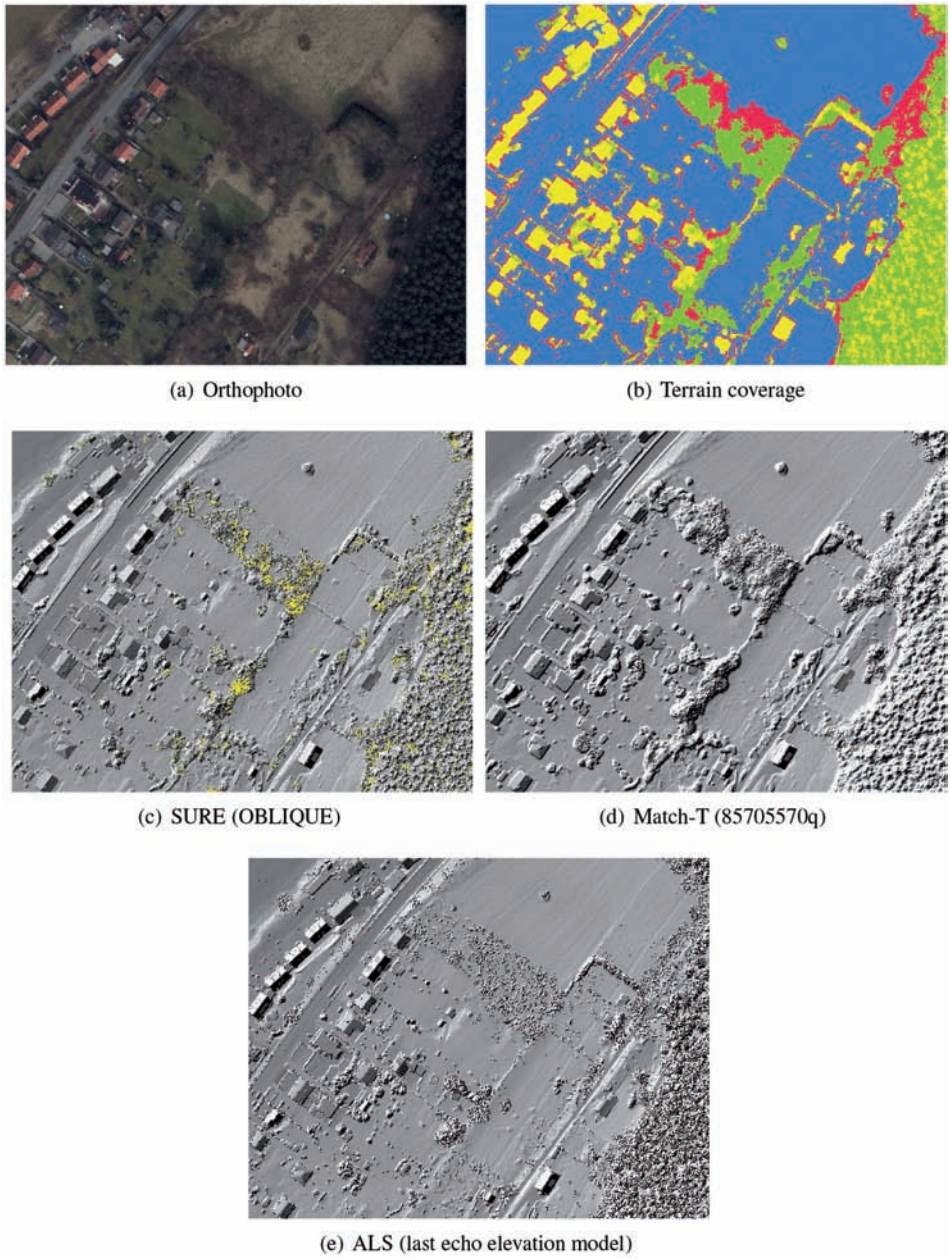

Fig. 9: Superimposition of the terrain coverages in the study area Weser (section). Blue: Match-T + SURE + ALS, red: SURE + ALS, green: ALS. Yellow = Off-terrain or masked. Additionally, the shadings of the respective grids are displayed. The east-west extension is about 330 m.

Tab. 2: Statistics of the height differences of all DIM variants in study area Weser with respect to the ALS-DTM in cm. The statistics of ALS tell how well the last echo points, which are classified as terrain, fit to the elevation model that was derived from them. All standard deviations refer to the mode, which is determined using a class width of 1.5 cm.

Method	Mean	Median	Mode	σ^-	σ^+	σ	RMS
ALS	0.4	0.2	-0.8	4.3	5.1	4.8	4.7
SURE (OBLIQUE)	3.5	2.5	0.8	5.0	7.7	6.9	7.1
SURE (DEFAULT)	4.8	3.2	0.8	5.1	8.0	7.2	7.5
SURE (AERIAL8080)	5.5	3.9	2.3	5.7	7.9	7.1	8.0
Match-T (UAS)	2.6	2.3	0.8	6.5	8.1	7.5	7.7
Match-T (85705570q)	3.1	2.2	0.8	5.2	8.0	7.0	7.3

for floating point samples can only be computed using classes. Here a class width of 1.5 cm was used. For all DIM variants the median is always below 4 cm and the mode is always below 2 cm. Thus, no considerable constant shift between ALS and the DIM results is present. The following three dispersion values refer to the mode.

- The standard deviation σ^-, which uses all ΔZ values within $[-20, 20]$ cm smaller than the mode. This value σ^- is representative for very smooth areas like sealed ground. For all DIM variants it is about 5 cm, which corresponds to half of the GSD.
- The standard deviation σ^+, which uses all ΔZ values within $[-20, 20]$ cm larger than the mode. Because the histogram in Fig. 6 is skewed to the right this value σ^+ will be larger than σ^- in general. It is representative for terrain showing a bit of roughness, e.g. grassland or (bare) forest floor. For all DIM variants it is about 8 cm.
- The standard deviation σ, which is computed using all ΔZ values within $[-20, 20]$ cm. This value is an average of the previous two and for all DIM variants it is about 7 cm.
- Finally, also the root-mean-square (RMS) of all ΔZ values within [-20, 20] cm is reported.

From Tab. 2 we see that SURE performs a bit better than Match-T and that the DIM statistics are only a little worse than the ALS results. From the RMS values we see, that the ALS points deviate by about 5 cm from the ALS-DTM, whereas the best DIM grid has a deviation of 7 cm.

4 Results for Study Area Elbe

For the second study area the very same methods as in section 3 were applied. Thus, only the main results are presented in the following.

4.1 *Terrain Classification*

A DTM is derived from the ALS data using all last echoes by means of a robust interpolation at a grid width of 0.5 m. Fig. 10 shows the histogram of the differences ΔZ of the last echoes to the DTM, limited to the interval abs(ΔZ) $<$ 20 cm. The ordinary standard deviation of these differences is 4.3 cm. The histogram is very similar to a Gaussian distribution. Based on that distribution the robust standard deviation σ_{MAD} is 3.9 cm and the median is 1.6 cm. The Gaussian distribution with these parameters is additionally drawn in Fig. 10, which fits to the histogram rather well, in contrast to the other study area Weser. This may be attributed to the very homogenous land cover, because 2/3 of study area Elbe are covered by grassland; see Fig. 2. In study area Weser the land coverage is much more diverse – especially the vegetation. All last echoes within $[-15, 15]$ cm are classified as terrain.

Fig. 11 shows the histogram of the DIM points of SURE (OBLIQUE) limited to $[-40, 40]$ cm. The median is 10.9 cm and σ_{MAD} is 5.4 cm. Compared to study area Weser (Fig. 5) two features are striking: (i) The Gaussian distribution using median and σ_{MAD} fits well to the histogram, which may be attributed again to the homogenous land cover. (ii) The median of 10.9 cm is significantly dif-

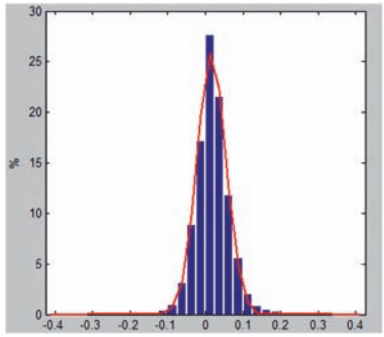

Fig. 10: Histogram of the height differences ΔZ (in m) of the last echoes to the ALS-DTM in study area Elbe; limited to abs(ΔZ) $<$ 20 cm. A Gaussian distribution with expectation 1.6 cm and standard deviation 3.9 cm is drawn in red.

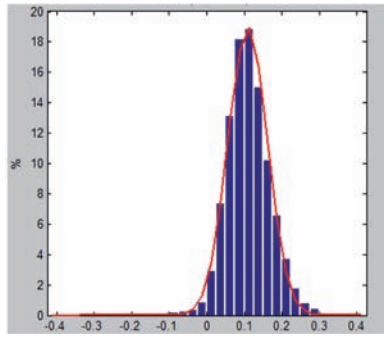

Fig. 11: Histogram of the height differences ΔZ (in m) of the SURE grid (OBLIQUE) to the ALS-DTM in study area Elbe; limited to abs(ΔZ) $<$ 40 cm. A Gaussian distribution with expectation 10.9 cm and standard deviation 5.4 cm is drawn in red.

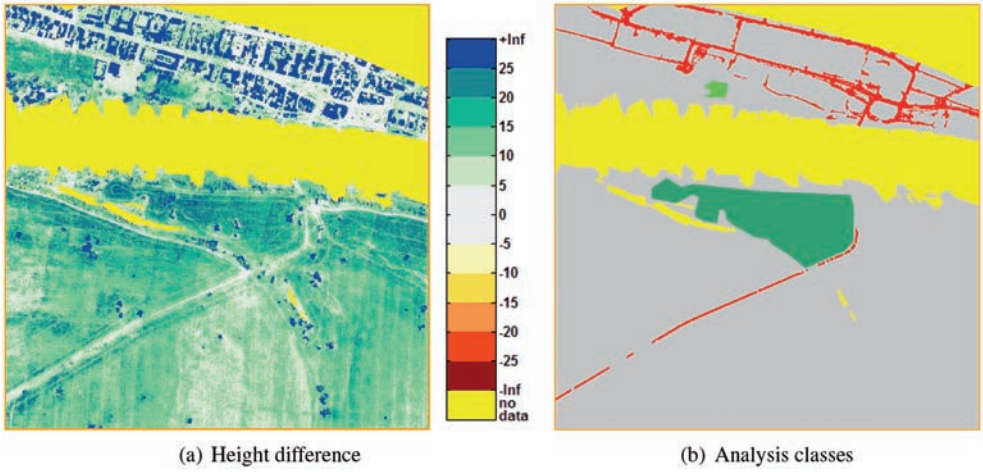

Fig. 12: Study area Elbe. Left: Colour coding of the height difference SURE (OBLIQUE) minus ALS-DTM. The colour table is in cm. Big differences only occur in grass land. At sealed surfaces (especially streets) small differences prevail. Right: Classes used for grass height analysis (red = sealed, bright green = vegetation 1, dark green = vegetation 2, grey = remaining data, yellow = no data).

ferent from zero (significance level 0.05). This is not caused by an error in the geodetic datum. A closer examination reveals that this constant difference of 10.9 cm only appears at grassland, but not at sealed surfaces; see Fig. 12a. Because ALS and images were acquired simultaneously, the only explanation can be the different penetration behaviours of ALS and images. Whereas the last ALS echoes may originate from deeper grass layers or even the terrain, the images only see the top of the grass.

Consequently, this leaves two options: Either we do not accept this height error and get no photogrammetric heights in about 2/3 of the study area, or we accept it and get terrain points which are at a wrong height. This second option is chosen and thus the DIM points are classified using the interval $[-10, 30]$ cm.

Tab. 3: Terrain coverage of the ALS and DIM points in study area Elbe. 'abs.' is the absolute count of raster cells classified as terrain. 'rel.' is this count in relation to the count of raster cells ($1.778 \cdot 10^6$) in the whole study area. The raster width is 75 cm.

Method	abs.	rel. [%]
ALS	1318092	74.1
SURE (OBLIQUE)	1298434	73.0
SURE (DEFAULT)	1290578	72.5
SURE (AERIAL8080)	1283998	72.2
Match-T (UAS)	1244494	69.9
Match-T (8060)	1241591	69.8

Tab. 4: Statistics of the height differences of all DIM variants in study area Elbe with respect to the ALS-DTM in cm. The statistics of ALS just tell how well the last echo points, which are classified as terrain, fit to the elevation model that was derived from them. The standard deviation refers to the mean. The modi were determined using a class width of 1.5 cm.

Method	Mean	Median	Mode	σ	RMS
ALS	1.9	1.6	-0.8	4.3	4.7
SURE (OBLIQUE)	8.8	10.9	9.8	6.3	11.9
SURE (DEFAULT)	8.7	11.3	11.4	6.4	11.9
SURE (AERIAL8080)	9.6	12.1	11.4	6.5	12.6
Match-T (UAS)	10.8	10.4	9.8	5.8	12.1
Match-T (8060)	11.9	12.1	12.9	5.4	13.4

4.2 *Terrain Coverage*

The terrain coverage is determined again as in section 3.3 using a raster with cell size 75 cm. We also consider a mask to exclude water and no-data areas from our analysis. Fig. 8b and Tab. 3 show the results. We see that for the whole study area ALS gives a terrain coverage of about 74 %, SURE 73 % and Match-T 70 %. Using the ALS result as reference, SURE delivers a quality of $73/74 = 98.5\,\%$, and Match-T a quality of $70/74 = 97.2\,\%$. In contrast to study area Weser, DIM performs quite close to ALS, which is due to the high percentage of open grassland in the study area.

The problem areas for DIM are the same as in study area Weser (see Figs. 8a and 9). In open areas SURE is able to deliver terrain heights closer to nearby off-terrain objects than Match-T (red areas in Fig. 8b). In dense or high vegetation areas, of which there are only a few in study area Elbe, only ALS can deliver terrain heights (green areas in Fig. 8b).

4.3 *Effect of Land Cover on Height Accuracy*

As in section 3.4 dispersion and location parameter are derived from the ΔZ values with respect to the ALS-DTM using the intervalls $[-20, 20]$ cm for ALS and $[-10, 30]$ cm for DIM; see Tab. 4. Since the histograms show no skewness at all only the ordinary standard deviation (with respect to the mean) and the RMS are given as dispersion values.

In section 4.1 the large offset of approximately 10 cm between DIM and ALS-DTM, which dominates also Tab. 4, was attributed to the different penetration behaviours of ALS and images. This offset is now analysed in two small areas of homogenous vegetation, which are shown in figure 12b in bright and dark green. They were selected using the orthophoto (Fig. 2) and the colour coded height difference (Fig. 12a). In order to judge this offset correctly any possible residual vertical datum error needs to be considered. Therefore, also the height differences in sealed areas are analysed, be-

Tab. 5: Statistics of the height differences of all DIM variants and the last echo points in study area Elbe with respect to the ALS-DTM in cm limited to sealed surfaces and two vegetation areas. The modi were determined using a class width of 1.5 cm.

Area	Method	Mean	Median	Mode	σ
sealed	ALS	2.8	2.6	3.0	5.5
	SURE (OBLIQUE)	4.8	4.7	3.8	3.0
	SURE (DEFAULT)	4.8	4.7	5.3	3.3
	SURE (AERIAL8080)	6.6	6.5	6.8	4.0
	Match-T (UAS)	5.6	5.5	5.3	4.5
	Match-T (8060)	5.6	5.4	5.3	3.6
vegetation 1	ALS	1.1	1.1	1.0	3.9
	SURE (OBLIQUE)	19.6	19.7	20.5	4.3
	SURE (DEFAULT)	20.8	20.9	20.5	4.6
	SURE (AERIAL8080)	18.2	18.4	18.9	4.7
	Match-T (UAS)	21.0	21.0	22.0	4.4
	Match-T (8060)	18.3	18.4	18.9	3.8
vegetation 2	ALS	2.1	2.1	1.0	4.3
	SURE (OBLIQUE)	16.4	16.8	17.4	5.5
	SURE (DEFAULT)	16.5	16.6	17.4	5.5
	SURE (AERIAL8080)	18.4	19.0	20.5	5.6
	Match-T (UAS)	17.2	17.9	20.5	5.7
	Match-T (8060)	17.5	18.2	20.5	5.2

cause there the penetration behaviours of ALS and images should be the same. The mask for the sealed areas (mostly asphalt) was digitized manually using the orthophoto and is shown in Fig. 12b in red.

Tab. 5 lists the ordinary standard deviation, the mean, the median and the mode (determined using class width 1.5 cm) for the ΔZ values of the ALS points and the DIM models with respect to the ALS-DTM within the sealed areas and the two vegetation areas. Because the location parameters, e.g. median, range between 3 cm and 20 cm, the median was computed first for the interval $[-10, 30]$ cm and afterwards the interval $[\text{median}-20, \text{median}+20]$ cm was used for computing the listed statistical values.

Despite the smooth nature of the sealed surfaces their ALS statistics are a little worse than the ALS statistics in the vegetation areas. This is attributed to the asphalt coverage in the sealed areas. According to the ASTER spectral library (Baldridge et al. 2009) the reflectance of near-infrared light for asphalt is around 10 %, whereas for green grass it is around 50 %. Consequently, the signal to noise ratio and thus the distance measurement accuracy for asphalt (5.5 cm) will be worse than for grass (3.9 cm and 4.3 cm, respectively).

Interestingly, for sealed surfaces the accuracy of the DIM variants (with respect to the ALS-DTM) is better than for ALS itself. Here it is important to point out that the ALS accuracy refers to the original last echo points, whereas the DIM accuracy refers to an interpolated grid. Additionally, the DIM variants employ some sort of smoothness constraint. This constraint can be exploited to the full at the sealed areas, because they are planar and horizontal to a large degree (and thus parallel to the image bases). Consequently, the smoothness constraint allows to bridge the asphalt parts with low texture by propagating the heights from objects with high texture, e.g. road markings.

Over the sealed surfaces the DIM variants show a small constant offset of about 5 cm, which may be attributed to a small remaining error in the datum of the images with respect to ALS. Over the vegetation areas both ALS and

DIM show similar standard deviations, but the location parameters are very different because of the different penetration behaviours.

The grass height in both vegetation areas can be estimated by subtracting the location parameter (mean, median or mode) in the sealed surfaces from the one obtained in each vegetation area. All three location parameters are very similar, as the underlying distributions are close to a Gaussian. Therefore, based on the results for SURE (OBLIQUE) the grass height can be estimated to be about 15.5 cm in vegetation area 1 and about 12.5 cm in vegetation area 2.

From the standard deviations listed in Tab. 5 we see that SURE and Match-T perform practically identical in both vegetation areas, and both DIM results are a little worse than ALS. In the sealed area SURE is a bit better than Match-T and reaches half of the GSD as standard deviation. There ALS is actually worse than DIM due to the low reflectance of asphalt. In the vegetation areas DIM delivers points on the top of the grass, which is about 10 cm above the terrain.

5 Conclusions

The topic of this study was the comparison of airborne laser scanning (ALS) and dense image matching (DIM) regarding their potential for deriving terrain heights. Two study areas were considered and their results are quite consistent. Only ALS can reliably detect the terrain beneath vegetation. State of the art DIM is currently only able to achieve this in areas with no or only very loose vegetation. In such areas SURE delivers somewhat better results than Match-T. This dependence on the vegetation density is primarily supported by the results of study area Weser. There the vegetation structure is very diverse with respect to, both, stem density and tree types. Consequently, DIM only achieved 78 % of the terrain that ALS detected. But study area Elbe also shows an interesting result: Even in the case of open grassland (where DIM reached 98.5 % of the terrain that ALS detected) the terrain heights obtained by DIM cannot be fully trusted. The ALS terrain heights were systematically lower by about 10 cm. It is concluded that DIM provides systematically wrong (too high) terrain elevations in such areas because matching occurs on top of the grass.

The very good height accuracy (as standard deviation) which can be achieved by DIM by exploiting the large image overlaps is encouraging. In both study areas the DIM height accuracy is only slightly worse than the ALS accuracy (6.5 cm vs. 4.5 cm). Specifically in smooth areas DIM can deliver heights with an accuracy of about half of the GSD.

Future developments in DIM may improve the matching quality of loosely vegetated terrain. However, because of the inherent occlusions caused even by leafless twigs, the terrain below loose vegetation will always be determined only by a small set of images with small base lines. Consequently, the reliability will be small and the height accuracy will be worse than presented here, where in the open areas the high image overlaps could be fully exploited.

Fig. 13: Dry fallen areas with groynes und groyne fields of river Rhine near Kaub.

On the other hand, in open areas with no or only very low grass coverage DIM can yield terrain data with high accuracy. Therefore, new possibilities arise for the BfG and the WSV, respectively, in the context of photogrammetric flights to be performed during periods of low discharge or for standardized high resolution mapping flights in dependence of given water levels and vegetation conditions. Ground data of groynes, groyne fields and other dry fallen areas of free flowing rivers, shown in Fig. 13, can be collected extensively on demand and efficiently with DIM. Furthermore, littoral zones can be captured at low water levels. These areas are difficult to collect by hydrographic measure-

ment systems, but they are predominantly open, supporting the use of DIM.

References

AdV, 2013: Leitfaden Qualitätsstandard Airborne Laserscanning (QS-ALS), Version 1.1. – AK-Beschluss 26/12 der 26. Tagung des Arbeitskreises Geotopographie der Arbeitsgemeinschaft der Vermessungsverwaltungen der Länder der Bundesrepublik Deutschland.

Baldridge, A.M., Hook, S., Grove, C. & Rivera, G., 2009: The ASTER Spectral Library Version 2.0. – Remote Sensing of Environment **113**: 711–715.

Baltsavias, E., 1999: A comparison between photogrammetry and laser scanning. – ISPRS Journal of Photogrammetry and Remote Sensing **54** (2–3): 83–94.

Bauerhansl, C., Rottensteiner, F. & Briese, C., 2004: Determination of terrain models by digital image matching methods. – International Archives of the Photogrammetry, Remote Sensing and Spatial Information Sciences **35** (Part B4): 414–419, Istanbul, Turkey.

Haala, N. & Rothermel, M., 2012: Dense multi-stereo matching for high quality digital elevation models. – PFG – Photogrammetrie, Fernerkundung, Geoinformation (4): 331–343.

Haala, N., Hastedt, H., Wolf, K., Ressl, C. & Baltrusch, S., 2010: Digital photogrammetric camera evaluation – generation of digital elevation models. – PFG – Photogrammetrie, Fernerkundung, Geoinformation (2): 99–115.

Hirschmüller, H., 2008: Stereo processing by semi-global matching and mutual information. – IEEE Transactions on Pattern Analysis and Machine Intelligence **30** (2): 328–341.

Kraus, K. & Pfeifer, N., 1998: Determination of terrain models in wooded areas with airborne laser scanner data. – ISPRS Journal of Photogrammetry and Remote Sensing **53**: 193–203.

Leberl, F., Gruber, M., Ponticelli, M. & Wiechert, A., 2012: The UltraCam story. – International Archives of the Photogrammetry, Remote Sensing and Spatial Information Sciences **39** (Part 1): 39–44, Melbourne, Australia.

Petzold, B., Reiss, P. & Stössel, W., 1999: Laser scanning – surveying and mapping agencies are using a new technique for the derivation of digital terrain models. – ISPRS Journal of Photogrammetry and Remote Sensing **54** (2–3): 95–104.

Rothermel, M., Wenzel, K., Fritsch, D. & Haala, N., 2012: Sure: Photogrammetric surface reconstruction from imagery. – Low Cost 3D Workshop.

Shan, J. & Toth, C.K. (ed.), 2008: Topographic Laser Ranging and Scanning: Principles and Processing. – CRC Press, Boca Raton, FL, USA.

Trimble, 2014: Match-T 5.5 Reference Manual.

Vastaranta, M., Wulder, M.A., White, J.C., Pekkarinen, A., Tuominen, S., Ginzler, C., Kankare, V., Holopainen, M., Hyyppä, J. & Hyyppä, H., 2013: Airborne laser scanning and digital stereo imagery measures of forest structure: Comparative results and implications to forest mapping and inventory update. – Canadian Journal of Remote Sensing **39** (5): 382–395.

Vosselman, G., Sester, M. & Mayer, H., 2004: Basic computer vision techniques. – J.C. McGlone (ed.). – Manual of Photogrammetry. American Society for Photogrammetry and Remote Sensing, chapter **6:** 455–504.

Wehr, A. & Lohr, U., 1999: Airborne laser scanning – an introduction and overview. – ISPRS Journal of Photogrammetry and Remote Sensing **54** (2–3): 68–82.

Xiao, J., Gerke, M. & Vosselman, G., 2012: Building extraction from oblique airborne imagery based on robust facade detection. – ISPRS Journal of Photogrammetry and Remote Sensing **68** (1): 56–68.

Zabih, R. & Woodfill, J., 1994: Non-parametric local transforms for computing visual correspondence. – Computer Vision ECCV '94, Lecture Notes in Computer Science, Vol. **801**, Springer Berlin Heidelberg, 151–158.

Addresses of the Authors:

Dr. Camillo Ressl, Technische Universität Wien, Department of Geodesy and Geoinformation, Gußhausstraße 27–29, A-1040 Vienna, Austria, e-mail: camillo.ressl@geo.tuwien.ac.at

Dipl.-Ing. Herbert Brockmann, Federal Institute of Hydrology, Department Geodesy, Am Mainzer Tor 1, D-56068 Koblenz, e-mail: brockmann@bafg.de

Dr. Gottfried Mandlburger, Technische Universität Wien, Department of Geodesy and Geoinformation, Gußhausstraße 27–29, A-1040 Vienna, Austria, e-mail: gottfried.mandlburger@geo.tuwien.ac.at

Prof. Dr. Norbert Pfeifer, Technische Universität Wien, Department of Geodesy and Geoinformation, Gußhausstraße 27–29, A-1040 Vienna, Austria, e-mail: norbert.pfeifer@geo.tuwien.ac.at

Manuskript eingereicht: September 2015

Angenommen: Januar 2016